Available online at www.sciencedirect.com
SCIENCE DIRECT®
PERGAMON
Vacuum 71 (2003) 491–496
VACUUM
SURFACE ENGINEERING, SURFACE INSTRUMENTATION & VACUUM TECHNOLOGY
www.elsevier.com/locate/vacuum

Reactive ion etching of Pt electrode using O_2-based plasma

Hyoun Woo Kim[a,*], Chang-Jin Kang[b]

[a] School of Materials Science and Engineering, Inha University, #253 Yong-Hyun-Dong, Nam-Ku, Incheon 402-751, South Korea
[b] Semiconductor R&D Center, Samsung Electronics, San#24 Nongseo-Ri, Kiheung-Eup Yongin-City, Kyungki Do 449-711, South Korea

Received 30 September 2002; received in revised form 3 March 2003; accepted 20 March 2003

Abstract

We have studied the reactive ion etching (RIE) of Pt electrode using O_2 plasma with additional gases. Dual frequency RIE tool was used to obtain a high-energy ion bombardment. We have investigated the Pt etching profile using O_2/HBr/Ar plasma. We reveal that there is a optimal gas flow ratio for attaining the node separation of Pt electrodes at small critical-dimension (CD) pattern.

Keywords: Pt; Etching; RIE; CD

1. Introduction

To increase a storage capacity per cell for 4 Giga-bit dynamic random access memory (DRAM) and beyond, the usage of barium strontium titanate (BST) capacitor has been considered and in the fabrication of ferroelectric random access memory (FRAM) device, the lead zirconium titanate (PZT) capacitor has been studied.

As an electrode material for both BST and PZT capacitors, various materials such as platinum (Pt), iridium (Ir), ruthenium (Ru), ruthenium oxide (RuO_2) and iridium oxide (IrO_2) have been chosen to be investigated. Among them, Pt is one of the most appropriate material because of its good oxidation-resistance, high electrical conductivity, and low leakage current [1].

Previous researchers have developed the Pt etching technique for patterning the bottom electrode in the stacked capacitor cell structure. However, as Pt has a low reactivity and most of its etching products have low vapor pressures [2,3], the etching of Pt proceeds by physical sputtering, resulting in low etch selectivity of Pt to mask and unwanted sidewall redeposition [4,5]. As a result, Pt has a low etch slope and thus the adjacent nodes are connected with Pt, the bottom Pt storage nodes cannot be separated from their adjacent storage nodes.

In order to solve this problem, we have tried to obtain a higher Pt etch slope with a higher Pt to mask etch selectivity [6]. By adopting a titanium (Ti) mask layer, which is not eroded significantly in O_2 plasma, and by employing the high temperature etching technique to promote the reaction of Ti mask layer and O_2 gas, we have attained an etch slope of 80°.

This work presents the result of research on the Pt electrode etching for 0.15–0.20 μm critical

*Corresponding author. Tel.: +81-32-860-7544; fax: +81-32-862-5546.
E-mail address: hwkim@inha.ac.kr (H.W. Kim).

0042-207X/03/$ - see front matter
doi:10.1016/S0042-207X(03)00074-5

dimension (CD) storage node pattern. We reveal that a reactive ion etching (RIE) lag occurs in case of Pt etching at a small-CD storage node pattern. We investigate the effect of the additive gas such as Cl_2, Ar, and HBr on the Pt etching characteristics. We also study the effect of those additive gases in order to surmount the RIE lag in Pt etching.

2. Experiments

The sample structures before and after opening hard masks are shown in Fig. 1. The sample structure was bottom SiO_2/titanium nitride (TiN) 500 Å/Pt 2000 Å/mask Ti 600 Å/mask SiO_2 3000 Å/photoresist. A storage node pattern was used in our experiments. Top view of the storage node pattern indicates that the storage node is an oval type.

The SiO_2 mask was patterned by $CF_4/CHF_3/Ar$ gas. After patterning SiO_2, which is a first mask for Pt etch, the photoresist was removed. The Ti layer, as a second mask for underlying Pt, was patterned by the Ar/Cl_2 chemistry using the SiO_2 mask.

Schematic of a RIE for Pt etching is shown in our previous work [6]. A dual frequency Tegal 6540 RIE tool commercially available from Tegal, Inc. has been used. The RF powers with a frequency of 13.56 MHz and 450 kHz were 500 and 300 W, respectively. In our Pt etching process, the chamber pressure was 6 m Torr and the total gas flow rate was 50 sccm, with the O_2 gas and additive gas flow rates of 40 and 10 sccm, respectively. The combination of high RF (HRF) power (13.56 MHz) and low RF (LRF) power (450 kHz), in addition to low pressure results in high-energy ion bombardment. The wafer substrate temperature during etching was measured to be about 220°C by combining 500 W of HRF power with 300 W of LRF power. The Pt etch process consists of a main etch step stopped at end point detection (EPD) and an 100%-over etch step to remove the Pt residues. Then the barrier TiN layer was removed by etching with Ar and Cl_2 gases.

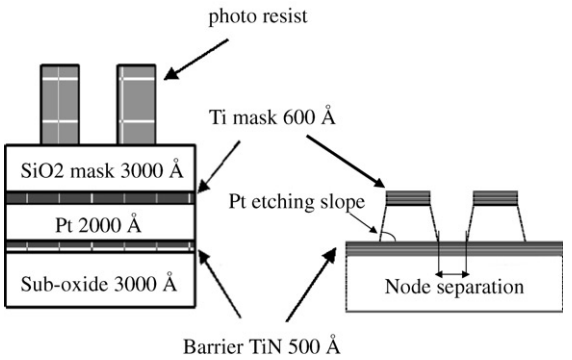

Fig. 1. Sample structure before and after opening SiO_2 and Ti hard mask. The sample structure is bottom SiO_2/titanium nitride (TiN) 500 Å/Pt 2000 Å/mask Ti 600 Å/mask SiO_2 3000 Å/photoresist.

After removing TiN barrier layer, the bottom space between two adjacent nodes should be wider than 80 nm, because the following steps of the BST deposition (estimated to be $\geqslant$300 Å in thickness per side) and the top electrode Pt deposition need to be accomplished. At the same time, the top width of the storage node should be maintained at about 0.15 μm to ensure a sufficient capacitance area and thus to satisfy a required storage capacity per cell. The required Pt etch slopes at the CD of 0.29 and 0.15 μm are calculated to be 67° and 82°, respectively. A scanning electron microscope (SEM) was used to evaluate the etched Pt electrode.

3. Results and discussions

We applied a high temperature Pt etching technique to stacked storage node pattern with a CD of 0.17 μm, with an expectation to apply the technique into future devices. The O_2/HBr mixture gas was used as an etchant. Top view of the storage node pattern indicates that the storage node is an oval type and space CDs along the short axis and the long axis are 170 and 280 μm, respectively. The left-hand side and the right-hand side of Fig. 2 show the vertical cross section of the storage node bottom electrode, along the short axis and the long axis, respectively. Along the long axis, the node has been separated by over etch, with the top Ti mask layer remained and the TiN bottom layer exposed. On the other hand, along

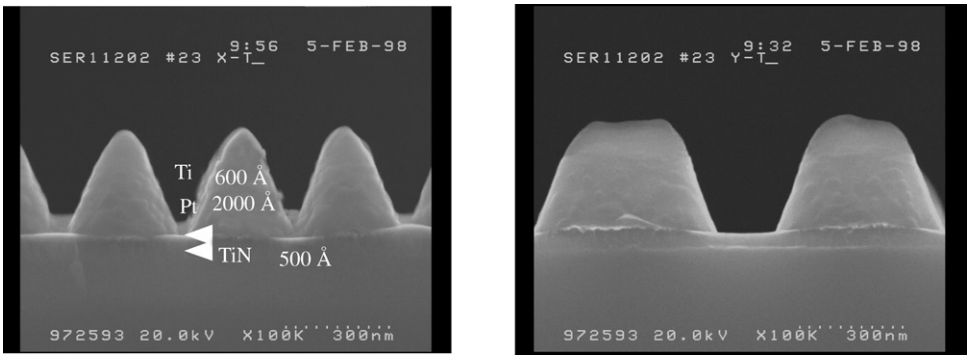

Fig. 2. Pt electrode profile with 100% overetch after EPD. The pre-etch CDs of the storage node pattern along the short axis and the long axis are 0.17 and 0.28 μm, respectively. Left: cross section along short axis. Right: cross section along long axis.

the short axis, the TiN bottom barrier is not exposed and the space CD is maintained to be zero even by excessive over etch, indicating that the Pt layer is connected along the short axis. Instead, the mask Ti layer is eroded in spite of the reaction with O_2 gas and the top part of the Pt node itself becomes etched and thus the height of the Pt storage node is reduced below 2000 Å. We surmise that the reduction of etch rate along the short axis results from the RIE lag. Because preliminary experiments indicated that the Pt etch rate is almost the same irrespective of additional gas, we surmise that the Pt etching process mostly consists of physical sputtering rather than chemical etching.

The RIE lag in Pt electrode etching is verified in Fig. 3, showing the Pt etch profile at the boundaries between the patterned and the unpatterned regions. While the etch slope towards the unpatterned region is about 80°, the etch slope towards the patterned region is below 70°. Due to the narrow space between adjacent storage nodes, both the reduction of the etch rate and the Pt etch slope occur coincidentally.

We investigated the change of Pt etching profiles at a storage node pattern with a CD of 0.20 μm using O_2/Cl_2, O_2/HBr, and O_2/Ar plasma. In this experiments, the O_2 flow rate is 40 sccm and the flow rate of additional gas is 10 sccm. Fig. 4 shows SEM micrographs of Pt etching profiles with additional gases of Cl_2, HBr, and Ar at the same etching condition. Close examination of the right-hand side of Fig. 4 indicates that the surface of the

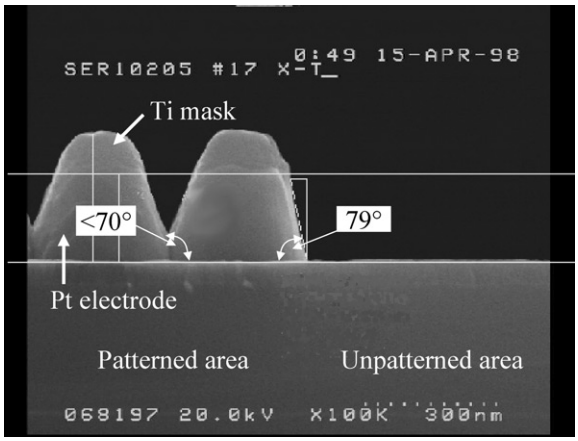

Fig. 3. Pt etch profile at the boundaries between the patterned and the unpatterned regions.

Ti mask layer is relatively smooth in case of using O_2/HBr system compared to O_2/Cl_2 and O_2/Ar systems. In case of O_2/Cl_2 and O_2/Ar system, the irregularities of Ti mask layer seem to be transferred to the underlying Pt electrode, resulting in a rougher Pt surface. The left-hand side of Fig. 4 indicates that the lengths of Ti mask layers along the long axis when etched with O_2/Cl_2 gas, O_2/HBr gas, and O_2/Ar gas are about 400, 410, and 500 nm, respectively, and thus the area of remaining Ti mask layer is larger in case of O_2/Ar systems than in other systems. We surmise that Ar does not erode the Ti mask layer as much as Cl_2 or HBr does, because the Ar does not chemically react with Ti layer. Most Ar species in plasma are

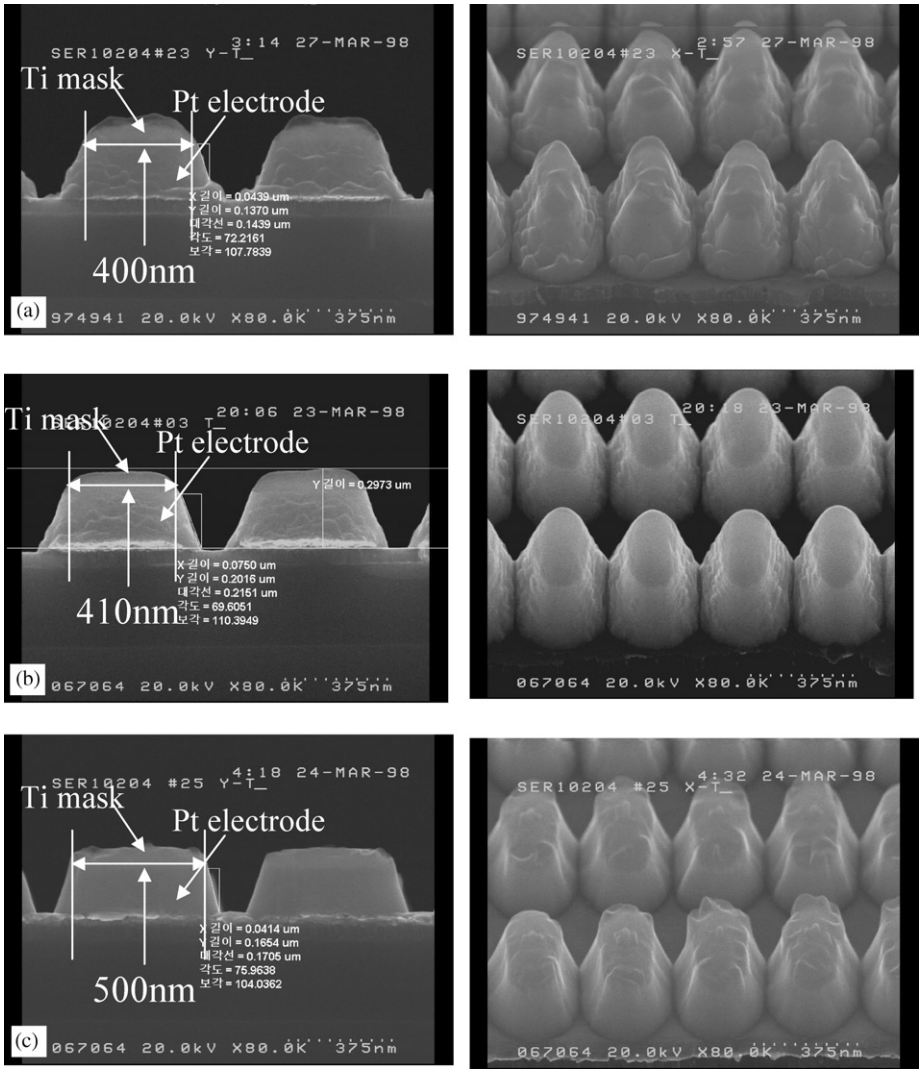

Fig. 4. SEM micrographs of Pt etching profiles using 40 sccm of O_2 gas with additional 10 sccm of: (a) Cl_2, (b) HBr, and (c) Ar at the same etching condition. Left: cross section along the long axis. Right: cross section along the short axis.

supposed to be used for physical sputtering and help to accelerate the reaction of Ti mask layer and oxygen species by elevating temperature. Although the Pt etching in RIE system proceeds mainly by physical sputtering, the Ti etching may proceed partly by chemical etching, resulting in the different morphology with different etching gas.

In order to improve the Pt etching profile at a small-CD pattern, we have employed the O_2/HBr/Ar plasma, because etching using O_2/HBr system results in smooth surface and etching using O_2/Ar system results in larger remaining Ti mask layer and thus higher Pt etching slope. The total flow rate is set to 50 sccm with an O_2 flow rate of 40 sccm. To study the effect of the CD, the storage node pattern with a CD of 0.20, 0.17, and 0.15 μm is used.

Fig. 5 shows the SEM images of Pt etching profiles depending on the Ar/(O_2 + HBr + Ar) gas flow ratio at a storage node pattern with a CD of

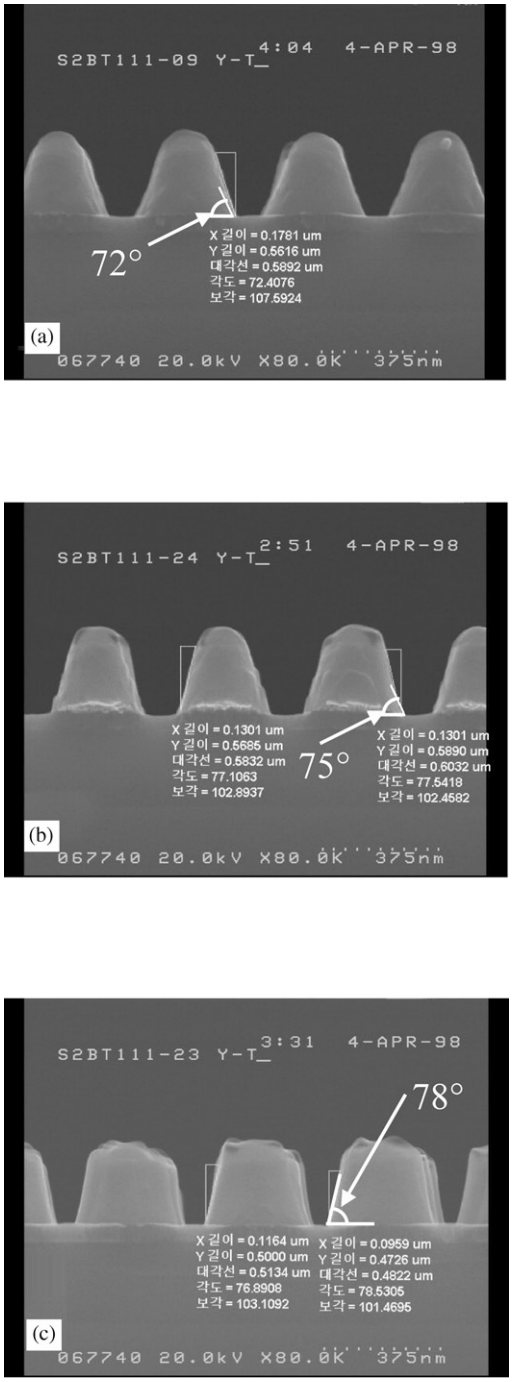

Fig. 5. SEM images of Pt etching profiles depending on the Ar/(O_2 + HBr + Ar) gas flow ratio at a storage node pattern with a CD of 0.20 μm. The O_2 flow rate is 40 sccm and the HBr and Ar flow rates are: (a) 7 and 3 sccm, (b) 5 and 5 sccm, and (c) 3 and 7 sccm, respectively.

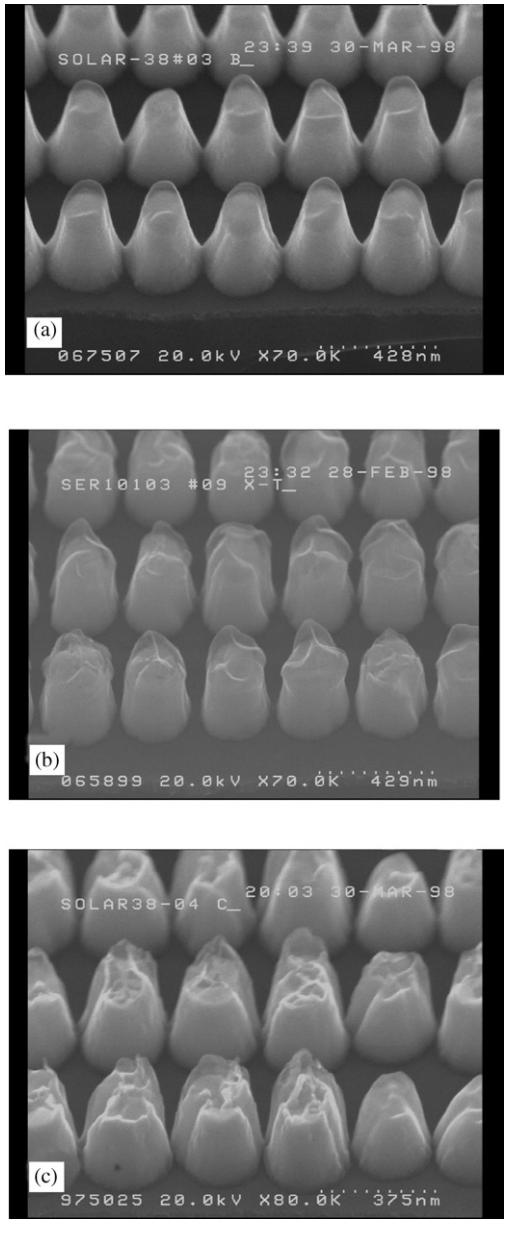

Fig. 6. SEM images of Pt etching profiles depending on the Ar/(O_2 + HBr + Ar) gas flow ratio at a storage node pattern with a CD of 0.15 μm. The O_2 flow rate is 40 sccm and the HBr and Ar flow rates are: (a) 7 and 3 sccm, (b) 5 and 5 sccm, and (c) 3 and 7 sccm, respectively.

0.20 μm. When Ar flow rates are 3, 5, and 7 sccm, respectively, the Pt etching slopes are 72°, 75°, and 78°, revealing that the Pt etching slope increases

with increasing $Ar/(O_2 + HBr + Ar)$ gas flow ratio. Close examination of tilted SEM images indicates that the erosion of Ti mask layer decreases and concurrently the deformation of Ti layer becomes significant with increasing $Ar/(O_2 + HBr + Ar)$ gas flow ratio. Previous study reveals that the increase of Pt etching slope is caused by the reaction of Ti mask layer with O_2 gas and thus the transformation of Ti mask layer into TiO_x layer [6]. According to the TEM analysis (not shown here), the volume of TiO_x layer when etched with a Ar flow rate of 7 sccm is bigger than that when etched with a Ar flow rate of 3 sccm. We surmise that Ar does not react chemically with Ti layer. Ar ions are supposed to be mainly used for physical sputtering and resulting heat helps to accelerate the reaction of Ti mask layer and oxygen species. More detailed study is necessary to reveal the role of Ar bombardment in enhancing TiO_x formation and thus elevating the Pt etching slope. The SEM images of Pt etching profile with a CD of 0.17 μm reveal that the Pt etching slope increase with increasing $Ar/(O_2 + HBr + Ar)$ gas flow ratio (not shown here).

Fig. 6 shows the SEM images of Pt etching profile with a CD of 0.15 μm, revealing that Pt has a low etching slope and thus the adjacent nodes are connected with Pt, the bottom Pt storage nodes cannot be separated from their adjacent storage nodes when etched with Ar flow rates of 3 and 7 sccm. However, it is noteworthy that the Pt storage nodes are separated and Ti mask layers are significantly transformed when etched with an Ar flow rate of 5 sccm. The average Pt etching slope at an optimal gas flow ratio at a CD of 0.15 μm is measured to be about 85°. This result differs from the result of 0.20 μm-CD pattern. More systematic study is needed to disclose an individual and combined effect of etchant gas.

4. Conclusions

We investigate the characteristics of Pt electrode etching using O_2-based plasma in reactive ion etcher. We reveal that the physical-sputtering nature of Pt etching is caused by RIE lag. It is shown that the etching characteristics of Ti mask layer using O_2/HBr and O_2/Ar is different. We study the characteristics of Pt etching using O_2/HBr/Ar plasma with varying gas flow ratio of Ar and HBr. We optimize the gas flow ratio of etchant gas for attaining high Pt etching slope at various CDs. We have obtained a Pt etching profile with its node separated at a CD of 0.15 μm.

Acknowledgements

The authors gratefully acknowledge financial support of present work by Semiconductor Research & Development Center of Samsung electronics Co. We especially thank to Dr. Moon Yong Lee and Dr. Joo Tae Moon for their advice. Also this work was supported by Inha University Research Grant through the Special Research Program in 2002.

References

[1] Saito S, Juramasu K. Jpn J Appl Phys 1 1992;31:135.
[2] Nishikawa K, Kusumi Y, Oomori T, Hanazaki M, Namba K. Jpn J Appl Phys 1993;32:6102.
[3] Yokoyama S, Ito Y, Ishihara K, Hamada K, Ohnishi S, Kudo J, Sakiyama K. Jpn J Appl Phys 1995;34:767.
[4] Yoo WJ, Hahm JH, Kim HW, Jung CO, Koh YB, Lee MY. Jpn J Appl Phys 1 1996;35:2501–4.
[5] Eimori T, Ono Y, Ito H. Nikkei Microdevices 1994;2:99.
[6] Kim HW, Ju BS, Nam BY, Yoo WJ, Kang CJ, Ahn TH, Moon JT, Lee MY. J Vac Sci Technol A 1999;17:2151–5.